



Magnetic plasma deorbit system for nano- and micro-satellites using magnetic torquer interference with space plasma in low Earth orbit

Takaya Inamori ^{a,*}, Rei Kawashima ^b, Phongsatorn Saisutjarit ^c,
Nobutada Sako ^d, Hiroyuki Ohsaki ^a

^a Department of Advanced Energy, The University of Tokyo, Tokyo, Japan

^b Department of Aeronautics and Astronautics, The University of Tokyo, Tokyo, Japan

^c King Mongkut's University of Technology North Bangkok, Department of Mechanical and Aerospace Engineering, Thailand

^d Canon Electronics INC, Tokyo, Japan

ARTICLE INFO

Article history:

Received 12 June 2014

Received in revised form

8 February 2015

Accepted 19 February 2015

Available online 28 February 2015

Keywords:

Nano- and micro-satellites

Deorbit

Space plasma

Magnetic torquers

Magnetic plasma deorbit

ABSTRACT

We propose a magnetic plasma deorbit (MPD) system using magnetic torquers (MTQs) for inducing the deorbit of nano- and micro-satellites. Currently, orbital space debris from these satellites is a matter of increasing concern to all satellites; however, deorbit systems have not been installed in most of these satellites. In general, nano- and micro-satellites have severe constraints on their power consumption, cost, and mass; therefore, it is difficult to install additional components that are not used in their main missions. The MPD system proposed in this study utilizes a drag force caused by the interaction between in-orbit space plasma and MTQs for attitude control. Because most nano- and micro-satellites already have MTQs installed for use in their attitude control, no additional thrusters and structures need to be installed for this deorbit system. Therefore, many satellites can be made to deorbit after their missions, which will reduce the accumulation of space debris. The present study assesses the duration required for the MPD to achieve deorbit using a plasma drag force model.

© 2015 IAA. Published by Elsevier Ltd. All rights reserved.

1. Introduction

Currently, nano- and micro-satellites are used for numerous types of missions, including remote sensing and astronomical observations [9,16]. Pico-satellite for Remote-sensing and Innovative Space Missions (PRISM) is an 8.5-kg nano-satellite that was launched in 2009 and successfully obtained 30-m-resolution images with an extendable telescope [10]. Nano-Japan Astrometry Satellite Mission for Infrared Exploration (Nano-JASMINE) is a 35-kg micro-satellite. The objective of its missions was to accurately estimate three-dimensional

star positions using star parallax. To achieve this mission objective, the satellite attitude had to be stabilized to an accuracy of 1 as [11]. As evidenced by these satellites, an increasing number of nano- and micro-satellites have been developed and launched into low Earth orbit (LEO) owing to their shorter development times and lower costs. In general, these satellites complete their missions in 1–10 years. However, most of these satellites maintain their orbit after their main missions are completed because they do not include any deorbit systems due to the strict constraints to mass and cost. Therefore, orbital space debris from these satellites is a matter of increasing concern for all satellites.

To prevent further accumulation of space debris, several deorbit systems have been proposed, most of which fall within two categories. The first category is satellite deorbit

* Corresponding author.

E-mail addresses: takayainamori@gmail.com,
inamori@space.t.u-tokyo.ac.jp (T. Inamori).

systems that use thrusters, such as ion engines. These systems are effective in deorbiting these satellites but require extra propellant and the installation of additional thrusters that are not necessary for the satellites' main missions. The second category is deorbit systems that use air drag forces. In this type of method, additional thrusters and propellant are not necessary, but additional structures with large areas are required to obtain strong drag forces. Both methods require the inclusion of additional components that are not used in the satellites' main missions but are installed only for deorbit after the completion of their main missions. In general, nano- and micro-satellites have severe constraints on their power consumption, cost, and mass; therefore, it is difficult to install additional components that are not required for their main missions, which is why such components have not been installed in many existing nano- and micro-satellites.

In this study, we propose a new method for nano- and micro-satellite deorbit using only magnetic torquers (MTQs) that are already installed in almost all nano- and micro-satellites as part of their attitude control systems, thus eliminating the need for additional parts. In general, there are many space plasma particles in LEO. Using the proposed deorbit method, the nano-satellite uses MTQs to generate a magnetic field that interacts with the space plasma and creates drag forces. In Section 2, we explain the basic concept of the proposed magnetic plasma deorbit (MPD) system. Using simplified models, we analyze the duration of MPD operation. In Section 3, we present our assessment of the proposed MPD method using numerical simulations. First, the drag forces are assessed using a plasma drag force model. Second, a satellite orbit during the MPD operation is calculated using the plasma model. Section 4 presents the primary conclusions drawn from this study.

2. Magnetic plasma deorbit

2.1. Basic concept of MPD

This section explains the basic concept of the proposed MPD method, an overview of which is given in Fig. 1. In LEO, space plasma caused by the Earth's atmosphere is present. In the proposed method, a nano-satellite uses MTQs to generate a magnetic wall that interacts with the space plasma in LEO and creates drag forces.

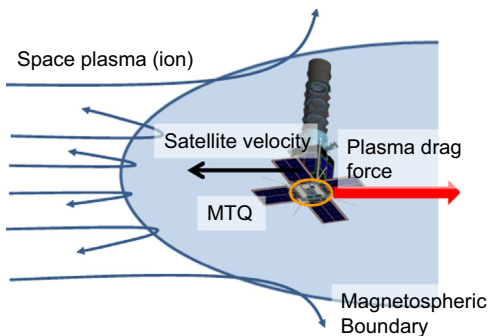


Fig. 1. Overview of magnetic plasma deorbit method using magnetic torquers (MTQs).

The drag forces caused by the interaction between a plasma flow and the magnetic moments of a satellite were previously investigated in magnetic plasma sails [6,7,8,17,20,22].

First, at the boundary, the internal magnetic pressure generated by an MTQ is equal to the external plasma pressure:

$$nm_i u^2 = \frac{(2B_{mp})^2}{2\mu_0}, \quad (1)$$

where n , m_i , and u are the plasma number density, ion mass, and plasma velocity, respectively. The parameter μ_0 is the vacuum permeability, and the parameter B_{mp} is the magnetic flux density at the boundary. In general, the magnetic flux density B at a distance L from the dipole center can be written as follows:

$$B_{mp} = \frac{M_d}{4\pi L^3}, \quad (2)$$

where the parameter M_d is the strength of the magnetic dipole moment. Here, the detachment distance of the boundary from the center of the magnetic dipole moment L can be written as follows:

$$L = \left(\frac{M_d^2}{8\mu_0 \pi^2 n m_i u^2} \right)^{1/6}. \quad (3)$$

This boundary, called the magnetopause, is where charged particles (ions and electrons) accumulate. The force on the current loop depends on the area blocking the plasma flow (πL^2). Thus, the plasma drag force F_p is expressed as follows:

$$F_p = -\frac{1}{2} C_{pd} \rho_p u^2 \pi L^2, \quad (4)$$

where ρ_p and C_{pd} are the plasma density and plasma drag coefficient, respectively. Eqs. (1)–(4) illustrate how larger magnetic moments generate larger magnetic walls, which in turn create larger drag forces.

To precisely calculate the plasma drag force, the effects of the satellite attitude and outer magnetic field should be taken into consideration. The relationship between the magnetic moment attitude and the strength of the magnetic drag force has been investigated in previous studies. From the results of these studies, the satellite can generate a plasma drag force in any attitude [2,19]. In the present study, we do not consider the attitude when performing a rough estimation. The plasma drag force in an outer magnetic field has also been investigated in several previous studies [21,19,17]. Furthermore, these study focused on interplanetary space craft using solar wind parameters. To roughly estimate the plasma drag force, the present study considers the plasma drag force without the outer magnetic field. Although these effects are not considered here, they should be investigated to obtain more precise estimations of the plasma drag force for LEO satellites. This concern will be explained in Sections 2–4.

The proposed MPD deorbit system is more effective in smaller satellites. First, we consider a cubic nano- or micro-satellite with edges of length l , and several similar satellites of different sizes are considered to analyze the scale dependency of the plasma drag force. In the case of the l -cm cubic satellite, the area S of a cubic plane of the satellite is $l^2 \text{ cm}^2$, and the satellite mass M is proportional to l^3 , as shown in

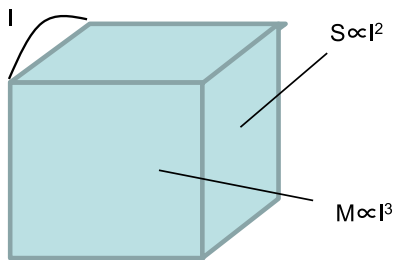


Fig. 2. Nano-satellite model used in the analysis of the plasma drag force effect.

Fig. 2. The maximum magnetic moment that this satellite can generate using an MTQ is assumed to depend on the area S of the satellite plane. In this case, the strength of the magnetic moment is proportional to the area S of the satellite panel. From Eqs. (3) and (4), the satellite drag force F is proportional to $M_d^{2/3}$; therefore, the relationship between the force and the satellite dimension l can be written as follows:

$$F \propto M_d^{2/3} \propto S^{2/3} \propto l^{4/3}. \quad (5)$$

This equation shows that the satellite can create a stronger force if the satellite size l is larger. From Eq. (5), the acceleration a of the satellite can be written as follows:

$$a \propto \frac{F}{M} \propto \frac{l^{4/3}}{l^3} \propto l^{-(5/3)}. \quad (6)$$

This equation shows that the satellite can generate a larger acceleration for orbit control if the satellite size is smaller. In this regard, the proposed MPD method is effective for smaller satellites, specifically for nano- and micro-satellites.

2.2. Estimation of deorbit duration using an analytical approach

To assess the proposed MPD method, it is important to understand the plasma environment in LEO. Thus far, most nano- and micro-satellites have been launched into LEO. Thus, this study considers the plasma environment in LEO using the International Reference Ionosphere (IRI) model. Fig. 3 shows the number density of electrons during daytime and nighttime and the composition of the in-orbit space plasma obtained by the IRI in 2012. In this model, the daytime and nighttime number densities are significantly different because the molecules in orbit are ionized by the sun during the daytime. In this model, most of the in-orbit plasma in LEO is O^+ , although the composition of the space plasma varies across days and nights. We assumed that the number density of the plasma is the same as the electron number density based on the assumption used in our analysis and numerical simulations that the in-orbit plasma is quasi-neutral.

To assess the effectiveness of the proposed MPD system in nano- and micro-satellite missions, we roughly estimated the deorbit duration using an analytical approach. The following points were assumed to simplify the analysis. First, the satellite orbit is assumed to be circular (eccentricity $e=0$). Second, the drag force generated by the MTQs does not affect any orbital parameters except the semi-major axis, and thus, the satellite maintains a circular orbit. Third, the space plasma

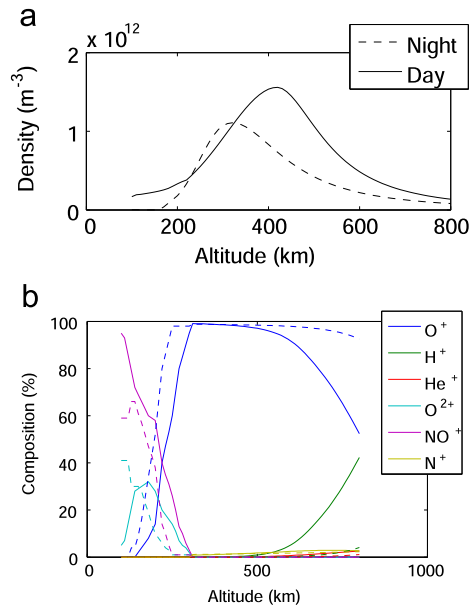


Fig. 3. (a) Altitude dependency of the electron density calculated by the International Reference Ionosphere (IRI) 2012 model. (b) Composition of the in-orbit space plasma calculated using the IRI 2012 model. The solid and dashed lines represent the composition of the plasma during the daytime (July 17, 2000, 0 h, Lat. 0°, Long. 0°) and nighttime (July 17, 2000, 0 h, Lat. 0°, Long. 180°), respectively.

in LEO is fed from neutral atmospheric particles, and the density of the plasma is constant in time. Finally, the dominant perturbation of the satellite orbit is caused by a plasma drag force. In this analysis, the orbital perturbation equation for the semi-major axis can be written as follows:

$$\frac{da}{dt} = \frac{2a^2 v F_p}{\mu m}, \quad (7)$$

where a , μ , v , and m are the orbital semi-major axis, standard gravitational parameter, satellite velocity, and satellite mass, respectively. Because the orbit is assumed to be circular, the satellite velocity can be expressed as $v = (\mu/a)^{0.5}$. F_p is the plasma drag force and can be expressed as in Eq. (4).

For the in-orbit plasma model, some particles in the atmosphere are ionized in-orbit and cause space plasma, but the total density of the space plasma is assumed to be constant in time. To obtain an analytical solution, the plasma density is assumed to be

$$\rho = \rho_r \exp\left(-\frac{a^{0.5} - a_r^{0.5}}{H}\right), \quad (8)$$

where a and H are the semi-major axis of the satellite orbit and a constant parameter, respectively. When modeling the atmosphere, the density is generally expressed as a function of altitude h as $\rho = \rho_r \exp(-(h-h_r)/H)$; however, this model cannot be integrated with respect to time in Eq. (7). Thus, in this study, we introduced another model for the atmosphere and expressed the density as a function of the semi-major axis, as in Eq. (8). The relationship between the IRI 2012 model and the proposed model given in Eq. (8) is illustrated in Fig. 4(a). In this figure, the plasma density is calculated using the number density of the plasma and the plasma

composition shown in Fig. 3. This comparison shows that the model in Eq. (8) is in agreement with the plasma density calculated by the IRI 2012 model when the altitude of the satellite is between 300 and 800 km. The plasma and air drag

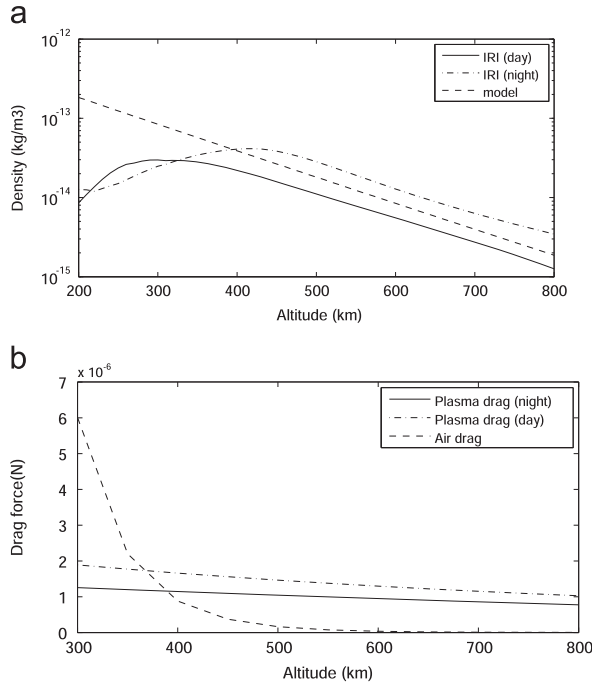


Fig. 4. (a) Plasma density calculated according to the International Reference Ionosphere (IRI) 2012 model and the model described by Eq. (8). (b) Plasma and air drag forces calculated according to the IRI 2012 and International Standard Atmosphere (ISA) models. In this calculation, the strength of an MTQ, the plasma drag coefficient, and the face area of the satellite are 30 A m², 1.0, and 0.01 m², respectively.

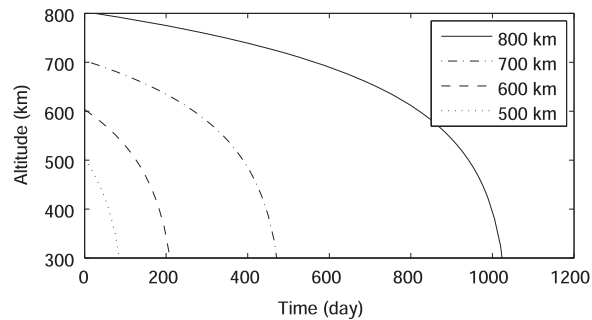


Fig. 5. Analytical results for descending trajectories achieved using the proposed MPD system.

Table 1
Parameters for the analysis shown in Fig. 5.

Item	Value
Reference semi-major axis: a_r	6900 km
Reference density: ρ_r	1.8×10^{-14} kg/m ³
H	25
Plasma drag coefficient: C_{pd}	1.0
Detachment distance of the boundary from the dipole center: L	3.3 m
Satellite mass: m	10 kg

forces acting on a satellite calculated according to the IRI 2012 and International Standard Atmosphere (ISA) models are illustrated in Fig. 4(b). As shown in Fig. 4(b), the plasma drag force is the dominant drag force when the satellite altitude exceeds 400 km. When the satellite altitude is between 300 and 400 km, the plasma and air drag forces have the same order of magnitude. In this study, we consider only the plasma drag force as the main source of drag force in Eq. (7), and thus, we only consider satellite altitudes exceeding 300 km.

From Eqs. (7) and (8), the semi-major axis during the MPD operation can be calculated as follows:

$$a = H^2 \ln \left(\frac{-C_d S \mu^{1/2} \rho_r (1/m) t + C_0}{2H} + a_r^{1/2} \right)^2, \quad (9)$$

where C_0 can be written as

$$C_0 = 2H \exp \left(\frac{a_0^{1/2} - a_r^{1/2}}{H} \right). \quad (10)$$

Here, a_0 is the initial altitude of the satellite. Fig. 5 shows an example of the calculation results obtained using the model described in the above equations. In this calculation, the satellite mass and the strength of an MTQ are 10 kg and 100 A m², respectively. During MPD operation, the satellite generates a steady magnetic moment and a drag force after its main mission is completed. Here, we consider the altitude of the satellite to be larger than 300 km, such that the main source of the drag force is the plasma drag force. At altitudes under 300 km, the dominant drag force is the air drag force, and the satellite re-enters the atmosphere within short period. Thus, the deorbit period is considered to be the period to reach an altitude of 300 km. The results given in Fig. 5 shows that the satellite completes deorbit within 2 years if the initial altitude is lower than 600 km. If the initial altitude is higher than 750 km, the satellite requires more than 5 years to deorbit because of the rarefied plasma environment. These results demonstrate that the proposed MPD method can be used to decrease satellite altitude and complete the deorbit of nano- and micro-satellites within several years (Table 1).

For the design of the MPD system, the estimation of MPD duration is important. The duration of the MPD operation t can be calculated from Eqs. (9) and (10) as follows:

$$t = \frac{2mH}{C_d S \mu^{1/2} \rho_r} \left(\exp \left(\frac{a_0^{1/2} - a_r^{1/2}}{H} \right) - \exp \left(\frac{a_{R_e}^{1/2} - a_r^{1/2}}{H} \right) \right), \quad (11)$$

where a_{R_e} is the Earth's radius. From this equation, the relationships between the deorbit duration, satellite mass, and magnetic moment of an MTQ can be estimated as

follows:

$$t \propto m,$$

$$t \propto S^{-1} \propto M_d^{-(2/3)}. \quad (12)$$

As shown in Eq. (12), the deorbit duration is proportional to the satellite mass and the 2/3 power of the magnetic moment $M_d^{2/3}$. From Eqs. (15) and (17) in Appendix A, the relationship between the magnetic moment and the mass of an MTQ is $M_d \propto M_{mtq}^{5/6}$. Thus, the deorbit duration is $t \propto S \propto M_{mtq}^{-5/9}$. In general, the mass of the MTQ is assumed to be limited by the satellite mass. Therefore, duration increases with larger satellite mass. Fig. 6 shows the satellite mass and magnetic moment dependencies of the MPD deorbit duration calculated by Eq. (11). This figure shows the required duration for the MPD operations using 1- to 300-A m² MTQs in 1- to 27-kg satellites when the initial altitude is 600 km. The two horizontal lines show durations of 2 and 4 years. Therefore, a 3-kg satellite can complete the MPD operation within 4 years using an 11-A m² MTQ, while a 9-kg satellite requires a 60-A m² MTQ to complete the MPD operation within 4 years.

2.3. Power consumption and mass of the MPD system

To assess the power consumption and mass of a MTQ, we introduce MTQ models proposed in previous studies, as shown in Appendix A. As a reference MTQ, we utilize the data for a large MTQ with experimentally confirmed parameters [15]. Lee et al. developed a 3-W, 5-kg MTQ and measured its magnetic moment using a magnetometer. From the results of their experiments, they concluded that the magnitude of the magnetic moment is 186 A m². To estimate the relationships between the mass, power consumption, and magnetic moment of an MTQ, we applied similar model introduced by a previous studies (Appendix A). Fig. 7 shows the relationship between the mass and power consumption of the magnetic torque and magnetic moment generated by an MTQ using the model given in Appendix A. These results show that a satellite can generate 11 A m² with a 0.3-kg, 1-W MTQ, which achieves the MPD operation shown in Fig. 5. Alternatively, the satellite can generate 60 A m² with a 1-kg, 5-W MTQ, which achieves a 4-year MPD in a 9-kg satellite. These MTQ masses and power consumptions are feasible in nano- and micro-satellite missions.

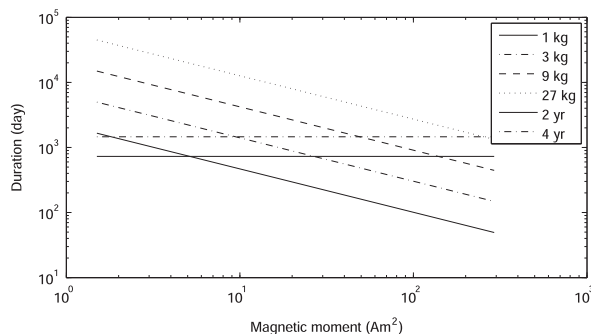


Fig. 6. Satellite mass and magnetic moment dependency of the MPD deorbit duration with an initial altitude of 600 km.

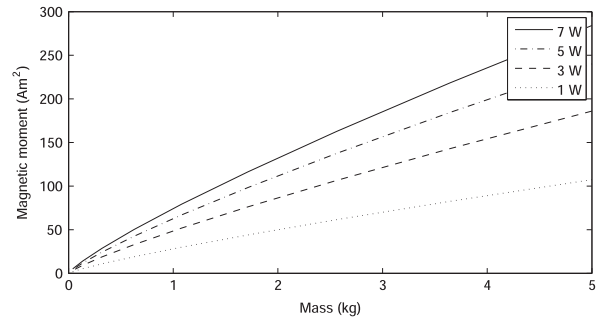


Fig. 7. Relationship between MTQ mass and the magnetic moment generated by the MTQ for various MTQ power consumptions.

2.4. Discussion of technical problems hindering the realization of MPD

Although the proposed MPD method has the potential to be a powerful technique for deorbiting LEO nano- and micro-satellites, there are several technical problems hindering its realization. Furthermore, the interaction between an artificial magnetic field and the space plasma in LEO is a phenomenon that has not yet been studied. These issues must be studied to realize MPD in the future. The following subsections summarize the primary technical issues that must be solved to realize MPD.

2.4.1. Effects of an outer magnetic field in LEO

Although the effect of the geomagnetic field is not considered in this study, the manner in which the outer magnetic field affects the plasma drag force was examined in previous studies [17,19,21]. These drag effects have been investigated in a solar wind environment. For a more precise estimation of the plasma drag force in LEO, this effect should be studied in an LEO environment. Furthermore, there are magnetic reconnection effects that are generated at a stable attitude in the geomagnetic field; this effect should be investigated to realize the proposed method.

2.4.2. Attitude control during an MPD operation

Attitude control during the proposed deorbit operations is an important issue. There are several potential deorbit methods regarding attitude control.

2.4.2.1. Deorbit without attitude control. In a previous study, the drag coefficient was shown to depend on the satellite attitude [2,19]. Although the drag force changes depending on satellite attitude, the plasma drag force is of the same in the order of magnitude at any attitude. Thus, the satellite can achieve deorbit without an attitude control system. In this case, the satellite attitude does not need to be stabilized with a large magnetic torque.

2.4.2.2. Deorbit with passive attitude control. During deorbit, the satellite has a large magnetic moment. In this system, the satellite can act as a magnet pointing along the direction of the geomagnetic field, like the passive magnetic attitude control system installed in some CubeSat satellites. In this case, the magnetic coil generates a large steady magnetic moment

for deorbit and attitude control and a small time-variable magnetic moment for attitude stabilization, which is similar to B-dot attitude stabilization. With this method, the satellite attitude can be stabilized and roughly controlled.

2.4.3. Magnetic material

The use of magnetic materials for a large MTQ in satellites has several effects on attitude control performance. First, magnetic material generally has a residual magnetic moment and thus causes magnetic disturbances. This effect can be countered by running a small flowing current through the installed magnetic coil for the deorbit system [12,13]. Second, the magnetic material affects the measurements of the magnetic sensor. Thus, if the requirements of the magnetic sensor are strict, it should be calibrated before use [1,4].

2.4.4. MTQs with large magnetic moments

There are several technical problems to overcome before the proposed MPD method can be realized. In the proposed MPD method, a strong magnetic moment should be generated using MTQs. Although the theory discussed in Appendix A holds that an MTQ with a large magnetic moment is technically possible, such MTQs need to be demonstrated in-orbit to realize their use.

2.4.5. Satellite lifetime

Furthermore, for the purposes of MPD, a satellite should be operable for several years after its main mission. In general, nano- and micro-satellites are developed using commercial off-the-shelf devices; thus, some satellites may be difficult to operate for several years. There are some examples of nano-

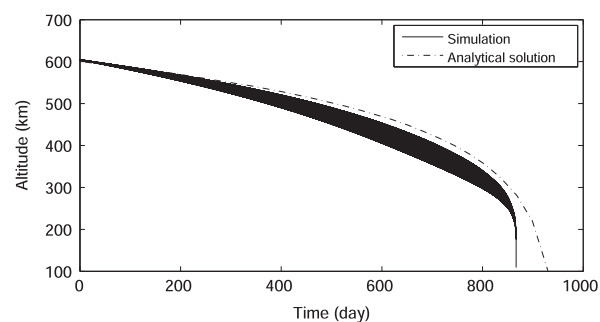


Fig. 8. Simulation results for satellite altitude during MPD operation with a 100-A m^2 MTQ in a 10-kg satellite (Satellite 1 in Table 2).

Table 2

Parameters for satellite simulations.

Item	Satellite 1	Satellite 2
Mass	10 kg	1 kg
Shape	20-cm cube	10-cm cube
Drag coefficient C_d for air disturbance	1	1
Drag coefficient C_{pd} for plasma drag	1	1
Orbit	Sun-synchronous orbit, LEO (initial alt. 600 km)	Sun-synchronous orbit, LEO (initial alt. 600 km)
MTQ	Magnetic dipole moment: 100 A m^2 Total mass: 2 kg Max power: 4 W Core: Ni-alloy Core dimension ($D \times L$): $16\text{ mm} \times 479\text{ mm}$ Coil turn number: 6546	Magnetic dipole moment: 5 A m^2 Total mass: 0.13 kg Max power: 1 W Core: Ni-alloy Core dimension ($D \times L$): $5\text{ mm} \times 142\text{ mm}$ Coil turn number: 6546

and micro-satellites that have had long lifetimes despite being designed to have short lifetimes. For example, CubeSats XI-IV and XI-V [18], developed at the University of Tokyo, are still working at the present time, approximately 10 years after their launches (2003–2014 and 2005–2014, respectively), although they were designed to have lifetimes of only several months. PRISM, developed by the University of Tokyo, is an 8.5-kg nano-remote sensing satellite that was launched in 2009 [14] and is also still functional (2009–2014). Although there have been missions in which satellites have operated for over 5 years, the satellite development requirements of a longer lifetime for deorbiting may increase satellite development cost. Thus, satellite lifetime should be discussed and studied to realize the proposed deorbit system.

3. Numerical simulations

To assess the duration of the proposed MPD method, we conducted an orbit simulation including a plasma model. We constructed a deorbit simulator using a simple geogravity model to assess MPD deorbit duration. In this simulation, we considered an air drag force calculated by the ISA model as a disturbance. For the plasma model, we utilized the IRI 2012 model [3], which calculates the ion number density and the composition of the plasma using the satellite position data and date. With the ion density data, the simulator calculates the plasma drag force according to the model obtained by Eq. (4). In these numerical simulations, the effect of the outer magnetic field is not considered. Thus, from the numerical simulations, we can roughly estimate the deorbit duration. The satellite position is updated using RK4 every 40 s. In this simulation, the satellite is in LEO with an initial altitude of 600 km. Fig. 8 shows the simulation results and the analytical solution for the satellite altitude during MPD operation with a 100-A m^2 MTQ in a 10-kg satellite (Satellite 1 in Table 2). The orbit is almost but not exactly circular, which is why the altitude changes periodically with the orbital frequency. Because the plasma density changes from day to night, as shown in Fig. 4, the drag force also changes with the orbital frequency. This periodic change of the drag force creates an elliptical orbit with a smaller eccentricity. This is why the amplitude of the altitude in an orbital period increases during the deorbit operation in Fig. 8. In this simulation, the satellite can be deorbited in fewer than 900 days, which is a shorter duration than that of the analytical result. This is because the aerodynamic drag force is modeled

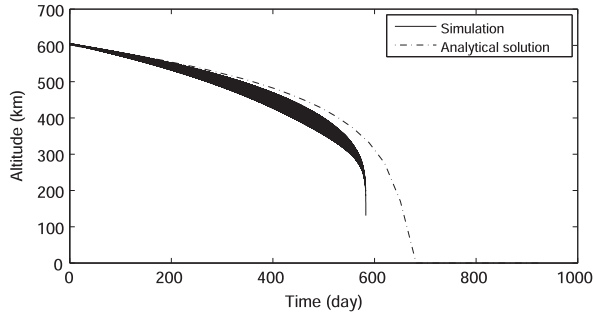


Fig. 9. Simulation results for satellite altitude during MPD operation with a 5-A m² MTQ in a 1-kg satellite (Satellite 2 in Table 2).

in this simulation. Furthermore, the altitude of the perigee decreases during MPD operation. Thus, the satellite is more strongly affected by aerodynamics and the plasma drag force, which makes the MPD operation period shorter. Fig. 9 shows the simulation results and the analytical solution for the satellite altitude during MPD operation with a 5-A m² MTQ in a 1-kg satellite (Satellite 2 in Table 2). In this simulation, the satellite can be deorbited after 600 days, which is a shorter duration than that of the analytical result, despite the fact that the strength of the contained MTQ is smaller than that in Satellite 1. These results demonstrate that the proposed MPD system is more effective in smaller satellites.

4. Conclusion

In this study, we proposed an MPD method for nano- and micro-satellite deorbit. Most existing nano- and micro-satellites do not include a deorbit system because they commonly implement strict limitations on mass, power consumption, and cost. Thus, it is not feasible to install additional systems used only for deorbiting after the completion of their missions. Our current study proposes the use of MTQs for deorbit. MTQs are already installed in almost all nano- and micro-satellites for their attitude control systems. In this system, the magnetic moment generated by the MTQs interacts with the space plasma in orbit and creates a drag force for deorbiting. According to the model of a plasma drag force, the plasma drag force generated by a 30-A m² MTQ is 5×10^{-0} N in a 1×10^{11} m⁻³ density plasma flow. Based on the simulation results using the IRI model, we developed an orbit simulator that includes the in-orbit plasma model under the assumption that there is no outer magnetic field. From the simulation results, a 10-kg satellite with a 100-A m² MTQ can complete its deorbit operation in 900 days from an initial altitude of 600 km.

Appendix A. Scale dependency of a magnetic moment generated by an MTQ

For the assessment of the MPD method, models of a magnetic torquer (MTQ) representing the relationship between the mass M , power consumption W , and magnetic moment

M_d is indispensable. This research utilizes experimental results and MTQ models in previous works. Although, in the previous works, several models have been proposed, it is difficult to find clear reason which model this study should choose [5,23]. Therefore, this study references experimental data of an MTQ whose specifications are similar to the MTQs utilized in this study and considers the relationship using similarity obtained by the model in the previous works. Ueshima introduced the following formula for the magnetic moment of an MTQ with a radius r and length l core [23]:

$$\begin{aligned} M_d &= B\pi r^2 l \mu_0^{-1}, \\ B &= \mu_0 \mu_{\text{eff}} n I l^{-1}, \\ \mu_{\text{eff}} &= \frac{1}{\mu} + \frac{\ln(l/r) - 1}{(l/r)^2} \end{aligned} \quad (13)$$

where I , n , and μ are the current of the coil, number of coil wiring, and magnetic permeability of the core, respectively. Meanwhile Fakhari introduced the following formula for the magnetic moment of an MTQ (Fakhari Mehrjardi and Mirshams [5]).

$$\begin{aligned} M_d &= \pi r^2 N I \left(1 + \frac{\mu_r - 1}{1 + (\mu_r - 1) N_d} \right), \\ N_d &= \frac{4(\ln(l/r) - 1)}{(l/r)^2 - 4 \ln(l/r)}. \end{aligned} \quad (14)$$

Here we consider the two similar MTQs whose geometric similarity is r/r_0 : the reference MTQ with the core radius r_0 , mass M_0 , power consumption W_0 , and magnetic moment M_{d0} ; and the focused MTQ with the core radius r , mass M , power consumption W , and magnetic moment M_d . These two MTQs are geometrically similar. In this case, the ratio l/r of the cores is the same in these two MTQs. First the relationship of the mass is proportional to the volume of the MTQs. Thus the relationship of the mass between two MTQs can be expressed as follows in the both Ueshima's and Fakhari's models:

$$M = \frac{r^3}{r_0^3} M_0. \quad (15)$$

As shown in the equation, the mass of the focused MTQ is proportional to the cubes of geometric similarity. Second, we consider the relationship of the power consumption between the two MTQs. Here the length of the electrical wire of the focused MTQ is $l_w = r/r_0 l_{w0}$. This is because the length of the wire is proportional to the core radius. Here it is notable that the number of coil wirings of the two MTQs is the same. Meanwhile the radius of the electrical wire σ is $r_w = r/r_0 r_{w0}$, thus the cross sectional area of the electrical wire of the focused MTQ is $S_w = r^2/r_0^2 S_{w0}$. Therefore, the electrical resistance σ is $\sigma = r_0/r \sigma_0$. In this case, to achieve the same power consumption in the two MTQs, the current of a wire is assumed to be $I = \sqrt{r/r_0} I_0$. Here, the power consumptions of the MTQs can be written as follows in the both Ueshima's and Fakhari's models:

$$W = W_0, \quad (16)$$

Finally, we consider the relationship of the magnetic moment between the two MTQs. In the both Ueshima's and

Fakhari's models, the magnetic moment is proportional to the squares of the core radius and currents. Thus the relationship of the magnetic moment is written as follows:

$$M_d = \frac{r^{2.5}}{r_0^{2.5}} M_{d0}, \quad (17)$$

As shown from Eqs. (15)–(17), the same similarity can be obtained in the both Ueshima's and Fakhari's MTQ models when the ratio l and r are the same, i.e., the MTQ is similar.

In the next step, we considered the magnetic moment of the reference MTQ with the different current I . The magnetic moment of the MTQ is proportional to the current in the both Ueshima's and Fakhari's MTQ models, thus the relationship can be written by:

$$M_d = \frac{I}{I_0} M_{d0}, \quad (18)$$

In this case, the power consumption is

$$W = \frac{I^2}{I_0^2} W_0. \quad (19)$$

From Eqs. (15)–(19), the relationship between the mass, power consumption, and magnetic moment of an MTQ can be calculated as shown in Fig. 7. For the reference MTQ, we utilize the data for a large MTQ (3-W, 5-kg, and 186 A m²) with experimentally confirmed parameters [15].

References

- [1] R. Alonso, M.D. Shuster, Attitude-independent magnetometer-bias determination: a survey, *J. Astronaut. Sci.* 50 (4) (2002) 453–475. Retrieved from.
- [2] Y. Ashida, H. Yamakawa, I. Funaki, Thrust evaluation of small-scale magnetic sail spacecraft by three-dimensional particle-in-cell simulation, *J. Propul.* 30 (1) (2014) 186–196. Retrieved from.
- [3] D. Bilitza, *International Reference Ionosphere 1990*, Greenbelt, Maryland, 1990, 0–84.
- [4] J.L. Crassidisy, K.-L. Laiz, Real-time attitude-independent three-axis magnetometer calibration, *J. Guid. Control Dyn.* 28 (1) (2005) 115–120.
- [5] Fakhari Mehrjardi, M., Mirshams, M. (2009). Design and manufacturing of a research magnetic torquer rod. (C. Quan, K. Qian, A.K. Asundi, F.S. Chau, (Eds.)), *Proc. of SPIE*, 7522. <http://dx.doi.org/10.1117/12.851652>.
- [6] K. Fujita, Particle simulation of moderately-sized magnetic sails, *J. Space Technol. Sci.* 20 (2) (2004). N/A–N/A.
- [7] I. Funaki, H. Kojima, H. Yamakawa, Y. Nakayama, Y. Shimizu, Laboratory experiment of plasma flow around magnetic sail, *Astrophys. Space Sci.* 307 (1–3) (2006) 63–68, <http://dx.doi.org/10.1007/s10509-006-9251-4>.
- [8] I. Funaki, H. Yamakawa, *Solar Wind Sails*, *Earth Planet. Sci. Astronom. Astrophys.* (2007) 439–462. In-Thech.
- [9] H. Heidt, J. Puig-Suari, A.S. Moore, S. Nakasuka, R.J. Twigg, CubeSat: a new generation of picosatellite for education and industry low-cost space experimentation, in: 14th Annual AIAA/USU Conference on Small Satellites, Logan, 2000. (2000).
- [10] T. Inamori, K. Shimizu, Y. Mikawa, Attitude stabilization for the nano remote sensing satellite PRISM, *J. Aerosp.* (2011) 594–602, [http://dx.doi.org/10.1061/\(ASCE\)AS.1943-5525.0000170](http://dx.doi.org/10.1061/(ASCE)AS.1943-5525.0000170). (Table 1).
- [11] Takaya Inamori, N. Sako, S. Nakasuka, Attitude control system for the nano-astronomy satellite "Nano-JASMINE", *Aircraft Eng. Aerosp. Technol.* 83 (4) (2011) 221–228, <http://dx.doi.org/10.1108/00022661111138639>.
- [12] Takaya Inamori, N. Sako, S. Nakasuka, Compensation of time-variable magnetic moments for a precise attitude control in nano- and micro-satellite missions, *Adv. Space Res.* 48 (3) (2011) 432–440, <http://dx.doi.org/10.1016/j.asr.2011.03.036>.
- [13] Takaya Inamori, N. Sako, S. Nakasuka, Magnetic dipole moment estimation and compensation for an accurate attitude control in nano-satellite missions, *Acta Astronaut.* 68 (11–12) (2011) 2038–2046, <http://dx.doi.org/10.1016/j.actaastro.2010.10.022>.
- [14] M. Komatsu, S. Nakasuka, University of Tokyo Nano Satellite Project "PRISM", *Trans. Jpn. Soc.* 7 (2009) 19–24. Retrieved from.
- [15] S.-H. Lee, H.-H. Seo, S.-W. Rhee, *Perform. Anal. Magn. Torquer Spacecraft Control* (2005). ICCAS2005 (Vol. 0).
- [16] F. Markley, Attitude determination using vector observations and the singular value decomposition, *J. Astronaut. Sci.* 38 (3) (1988) 245–258. Retrieved from.
- [17] M. Matsumoto, Y. Kajimura, H. Usui, I. Funaki, I. Shinohara, Two-dimensional hybrid-PIC simulation of magnetic sail including interplanetary magnetic field, *J. Jpn. Soc. Aeronaut. Space Sci.* 60 (1) (2012) 31–39, <http://dx.doi.org/10.2322/jjsass.60.31>.
- [18] S. Nakasuka, N. Sako, H. Sahara, Y. Nakamura, T. Eishima, M. Komatsu, Evolution from education to practical use in University of Tokyo's nano-satellite activities, *Acta Astronaut.* 66 (7–8) (2010) 1099–1105, <http://dx.doi.org/10.1016/j.actaastro.2009.09.029>.
- [19] Nishida, H., Funaki, I. (2010). Aerodynamic characteristics magnetic sail in magnetized solar wind. in: 61th International Astronautical Congress, Prague, CZ. Retrieved from (<http://scholar.google.com/scholar?hl=en&btnG=Search&q=intitle:AERODYNAMIC+CHARACTERISTICS+OF+MAGNETIC+SAIL+IN+MAGNETIZED+SOLAR+WIND#0>).
- [20] Nishida, H., Ogawa, H., Funaki, I., Fujita, K. (2005). Verification of momentum transfer process on magnetic sail using MHD Model. in: 41st AIAA/ASME/SAE/ASEE Joint Propulsion Conference & Exhibit. Tucson, Arizona. Retrieved from (<http://arc.aiaa.org/doi/pdf/10.2514/6.2005-4463>).
- [21] Hiroyuki Nishida, R. Nagai, I. Funaki, Characterization of effects of interplanetary magnetic field on thrust force of magnetic sail, *Proc. Space Sci. Technol. Conf.* (2009). Kyoto.
- [22] Hiroyuki Nishida, H. Ogawa, I. Funaki, Two-dimensional magneto-hydrodynamic simulation of a magnetic sail, *J. Spacecraft* 43 (3) (2006) 667–672, <http://dx.doi.org/10.2514/1.15717>.
- [23] Ueshima, H. Attitude control system and magnetic torquer for the Hokkaido satellite; 2005. Retrieved from (<http://www.hit.ac.jp/~satori/labo/ronbun/h16-1.pdf>).